AIAA 98-0589

The NASA-Langley Wake Vortex Modelling Effort in Support of an Operational Aircraft Spacing System

Fred H. Proctor
NASA Langley Research Center
Hampton, Virginia

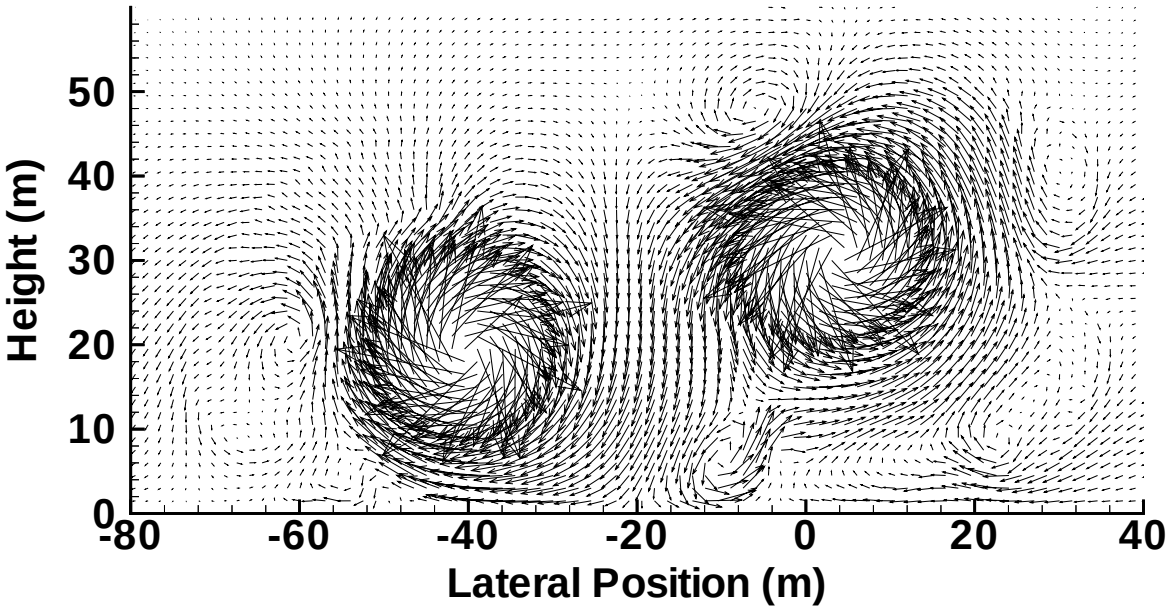

36th Aerospace Sciences Meeting & Exhibit
January 12-15, 1998 / Reno Nevada

AIAA-98-0589

The NASA-Langley Wake Vortex Modelling Effort in Support of an Operational Aircraft Spacing System

Fred H. Proctor*
NASA Langley Research Center
Flight Dynamics & Control Division
Hampton, VA 23681-0001

Abstract

Two numerical modelling efforts, one using a large eddy simulation model and the other a numerical weather prediction model, are underway in support of NASA's Terminal Area Productivity program. The large-eddy simulation model (LES) has a meteorological framework and permits the interaction of wake vortices with environments characterized by crosswind shear, stratification, humidity, and atmospheric turbulence. Results from the numerical simulations are being used to assist in the development of algorithms for an operational wake-vortex aircraft spacing system. A mesoscale weather forecast model is being adapted for providing operational forecast of winds, temperature, and turbulence parameters to be used in the terminal area.

This paper describes the goals and modelling approach, as well as achievements obtained to date. Simulation results will be presented from the LES model for both two and three dimensions. The 2-D model is found to be generally valid for studying wake vortex transport, while the 3-D approach is necessary for realistic treatment of decay via interaction of wake vortices and atmospheric boundary layer turbulence. Meteorology is shown to have an important affect on vortex transport and decay. Presented are results showing that wake vortex transport is unaffected by uniform fog or rain, but wake vortex transport can be strongly affected by nonlinear vertical change in the ambient crosswind. Both simulation and observations show that atmospheric vortices decay from the outside with minimal expansion of the core. Vortex decay and the onset three-dimensional instabilities are found to be enhanced by the presence of ambient turbulence.

Nomenclature

B	aircraft wingspan
b_o	initial vortex separation
g	acceleration due to gravity
N	Brunt-Vaisala frequency
N^*	$N\, b_o/V_o$
Re_r	Reynold's number based on circulation
r	radius from vortex center
r_c	radius of peak tangential velocity
t*	t Vo / b_o
t	time
U	ambient crosswind
V	tangential velocity
V_a	true airspeed
V_o	$\Gamma/(2\,\pi\, b_o)$
W	mass of aircraft
z	vertical coordinate
Γ	circulation
Γ_∞	circulation at large r (total circulation)
ρ	air density
ϵ	turbulence (eddy) dissipation rate
ϵ^*	$(\epsilon b_o)^{1/3}\, V_o^{-1}$
ν	kinematic viscosity
ω	vorticity due to vertical shear of crosswind

*Research Scientist, AIAA member

I. Introduction

For the purpose of increasing airport capacity, a system is being developed under NASA's Terminal Area Productivity (TAP) program that will control aircraft spacing within the narrow approach corridors of major airports. The system, called the Aircraft Vortex Spacing System (AVOSS),[1, 2, 3, 4] will determine safe operating spacings between arriving and departing aircraft based on the observed/predicted weather state. This system should provide a safe reduction in separation of aircraft compared to the now-existing flight rules, which are conservatively-based on aircraft weight categories. The existing flight rules are applied only during instrument flight conditions, and otherwise, do not depend on the current or anticipated weather state. The inclusion of atmospheric state variables would reduce the separations needed for safe flight since crosswinds may transport the aircraft wake vortices outside of the narrow terminal-area flight corridor and since significant levels of atmospheric turbulence may enhance the demise of the vortices.

As part of the TAP program, two numerical modelling efforts are in progress. A nonhydrostatic compressible numerical model is being used to investigate relationships between the atmospheric state and wake vortex behavior. This numerical modelling effort will be described in section III. It is not our intention to use this model as an AVOSS predictor, but to provide useful relationships between weather and vortex behavior. Information provided by this effort, along with data from field studies, will contribute to the development of a simple semi-theoretical/empirical predictor algorithm[5] for AVOSS. The second numerical modelling effort involves tailoring a preexisting hydrostatic, mesoscale weather-forecast model for short-term predictions of weather conditions that might be needed for the AVOSS system. This effort will be briefly described in section II. The numerical modelling efforts are being performed at NASA Langley, with major contributions from: two cooperative agreements with North Carolina State University's (NCSU) department of Marine Earth and Atmospheric Sciences, a grant with University of South Alabama's department of Mechanical Engineering, and a task contract with Research Triangle Institute (RTI).

Since atmospheric effects are anticipated as having a strong influence on wake vortex behavior, extensive meteorological measurements were made during the recent NASA sponsored deployments at Memphis[6, 7] and at the Dallas-Ft. Worth (DFW) International airports. Environmental data was obtained from a variety of sensors that included a 42 m instrumented tower, an acoustic sodar, an atmospheric wind profiler, a radio acoustic sounding system (RASS), soil temperature and solar radiation sensors, and special rawinsonde balloon launches. During these deployments, wake vortices generated by routine air traffic were measured by MIT-Lincoln's 10.6 micron continuous wave coherent laser (Lidar).[8] In addition, a pulsed-Doppler Lidar developed under contract at NASA Langley,[9] has recently become operational and was deployed at DFW during the late summer of 1997. The data generated from these deployments is believed to be the most comprehensive to date of any wake-vortex field study, and will be used to develop and test engineering models, as well as to validate the numerical modelling efforts.

Meteorological Effects

Meteorology has long been believed by many to play a significant role on wake vortex behavior. Previous field studies of aircraft wake vortices conducted over the past 25 years,[10, 11, 12, 13] as well as the recent NASA deployments have shown important atmospheric influences.

Atmospheric effects on aircraft wake vortices can be divided into two categories: transport and decay. The latter has attracted the most interest from researchers. However, understanding and quantifying how wakes transport (both vertically and horizontally) in various atmospheric flows is crucial to the development of an AVOSS system.

Crosswinds cause vortices to drift in the direction of the crosswind. Thus, wake vortices generated in the presence of a significant crosswind may have a relative short residence time in the aircraft approach corridor. Based on data from field measurements, Hallock[14] reported that aircraft spacing between the threshold and middle marker could be reduced uniformly to 3 nautical miles for all aircraft types, if the surface-level crosswind component was greater than 3.8 m/s (7.5 knots). A precise prediction of the lateral transport of vortices is made more difficult by the nonuniform variation of wind speed and direction with both altitude and time.

The transport of wake vortices is further complicated by their groundward descent. Two dominant trailing vortices are formed behind each aircraft and

descend due to their mutual induction. Wake vortices initially descend at a speed based on the generating aircraft's weight, airspeed, and wingspan. This descent velocity may change with time due to ambient thermal stratification, ambient windshear, and the decay of the vortices. Vertical wind associated with phenomena such as vigorous fronts, gravity waves, and large-scale atmospheric turbulence (such as thermal plumes), may also effect the descent of vortices. Rising vortices have been observed that cannot be explained by surface rebound.[15, 16] Vertical shear of the crosswind component can affect the descent of wake vortices and in some cases cause them to rise.[17, 18] The influence of crosswind shear on vortex trajectory is being examined from our numerical modelling effort and will be described later in this paper.

The decay of vortices has been somewhat controversial.[19] Numerous researchers in academia and industry believe that vortices generally do not decay until some stochastic event causes their sudden demise.[20, 21] This view is held in light of overwhelming observational evidence that vortices decay at a rate dependent upon the ambient meteorology. Atmospheric turbulence eats away at vortices eroding them form the outside,[22, 23] and may accelerate the development of three-dimensional instabilities that quickly dissipate the strength of the vortices.[24] During our NASA deployments, Lincoln's Lidar was able to track vortices for up to several minutes during the evening and early AM hours when atmospheric turbulence levels were light; but during daylight hours when turbulence was more vigorous, they found that vortices would often dissipate within about ½ minute.[25] Tombach[10] notes that although there is a strong correlation between atmospheric turbulence and vortex lifetime, a weaker but apparent correlation exists between vortex lifetime and lapse rate for temperature. Vortex descent through a stably-stratified atmosphere would generate counter-sign vorticity along the vortex oval's periphery which could hasten vortex decay. Given these observations and deductions, we might expect that the most persistent vortex to occur in an environment with minimal turbulence and near neutral stratification. These deductions are qualitatively consistent with the vortex decay model formulated by Greene[26] which resides as a key ingredient of the AVOSS predictor algorithm.

Figure 1 which is adapted from Stull's fig. 1.7,[27]

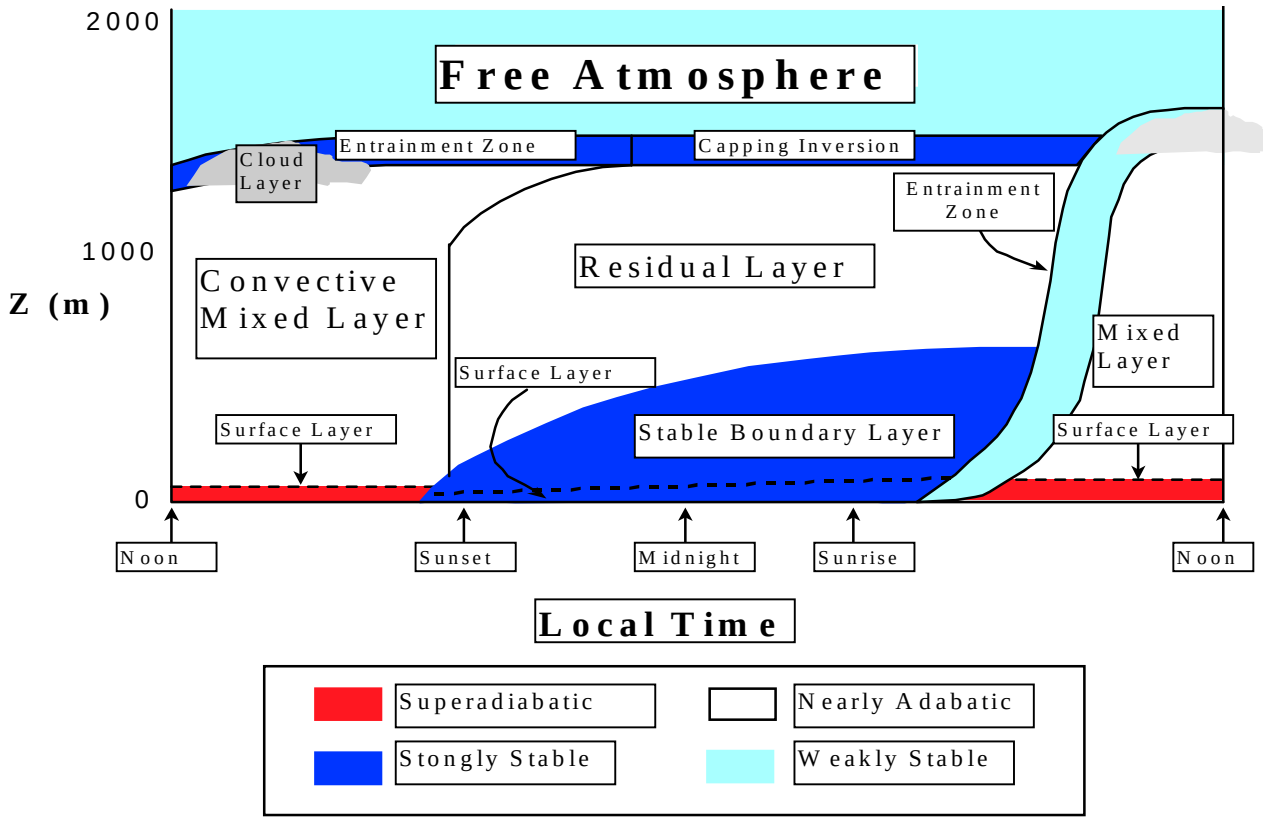

Figure 1. *Diurnal variation of the earth's boundary layer over land (courtesy of Dave DeCroix).*

shows the typical diurnal evolution of the atmospheric boundary layer during fair weather conditions. Shortly after sunrise solar radiation causes the ground to heat up rapidly, forming a deep convective mixed layer that persists until sunset. The properties of this layer are near neutral stratification (lapse rate) and nearly uniform wind speed and direction. Strong turbulence, with a maximum length scale equivalent to the depth of the mixed layer, is driven by the surface heating. When present, the base of cumulus clouds are a visual indicator of the mixed layer's depth. The convective mixed layer is separated from the ground by a surface layer that has a depth of tens of meters. During daytime hours, unstable lapse rates and most of the atmospheric boundary-layer shear are found in the surface layer. Wake vortices generated in the convective mixed layer should have relatively short lifetimes due to the large intensity of turbulence. After sunset, the ground radiates its heat into space and cools the layer of air immediately above. This leads to the development of a nocturnal stable boundary layer, which grows during the evening hours and reaches a maximum depth around sunrise, of only a few hundred meters. The air within this layer usually has weak wind speeds and minimal (although sporadic) turbulence. The turbulence that exist in this layer is generated mechanically by wind shear and flow over obstacles. Above the stable boundary layer is a residual layer which has similar properties to the convective mixed layer that was present earlier in the day. However, the residual turbulence is no longer supported by surface heating and is weakening with time. Lapse rates for temperature are quite stable in stable boundary layer but near neutral in the overlaying residual layer. Nocturnal jets of air are sometime present just above the interface between the stable and residual layers. Wake vortices generated in the residual layer may persist due to the near neutral stratification and weak to moderate turbulence. However, as the wakes descend, they may be deflected by strong vertical shear near the layer interface. Since atmospheric turbulence levels are minimal within the stable boundary layer, wake vortices should persist, even though stable stratification and the interaction with the ground would act to enhance their rate of dissipation. Wake vortices generated above the boundary layer in the free atmosphere would usually decay slowly in stable stratification and weak turbulence. In the scenario shown in fig. 1, wake vortices may be expected to persist the longest within the residual layer (some time after sunset), and decay the quickest in the surface and convective mixed layer. Since atmospheric properties in the stable layer are usually quite different from that in the residual layer, wake vortices generated in the residual layer between sunset and sunrise may be poorly predicted from atmospheric measurements, of atmospheric properties near the ground.

The idealized behavior of the diurnal variation of the atmospheric boundary layer, as described above and depicted in fig. 1, is made more complicated by the effects of cloud cover, fronts, and other synoptic and mesoscale events in the atmosphere.

The maximum range of turbulence length scales varies between atmospheric layers, usually being largest within the mixed boundary layer. In this layer, atmospheric turbulence has an inertial subrange extending to scales equivalent to the depth of the boundary layer.[27] This means that there is a continuous spectrum of eddy sizes extending to as large as 1 to 3 km – a value which is almost two-orders of magnitude larger than the initial vortex separation (b_o) produced by most aircraft. Scales of turbulence less than b_o can lead to enhanced diffusion of vortex circulation,[28] while scales between b_o and 10 b_o are most likely to trigger the development of Crow instability.[29] Scales of turbulence larger than b_o would also act to transport, stretch and deform wake vortices. Oddly, turbulence must be considered in the *transport* algorithm of an AVOSS predictor model, since atmospheric boundary layer turbulence may act to transport as well as decay vortices. For example, a vortex trajectory prediction based on mean crosswind becomes less precise in an active mixed layer.

Wake Vortex Structure and Decay Mechanisms

Typical Reynold's numbers ($Re_r = \Gamma_\infty/\nu$) for atmospheric wake vortices are on the order 10^7, implying that the effect of molecular diffusion is inconsequential. With this value, the decay of an atmospheric wake vortex by diffusion alone would take about 10 hours.[23] In reality, wake vortices in the atmospheric boundary layer last several minutes at the most, with the principal decay mechanism attributed to both ambient and self-generated turbulence.

Turbulence is strongly affected by the rotation of a swirling flow, which in turn, affects the structure of that flow. According to Rayleigh's well-known stability criterion, perturbations are suppressed in an axisymmetric vortex if the circulation is increasing with radius, but, perturbations would become unstable if the circulation is decreasing with radius. In the stable case, both centrifugal force and radial pressure gradient act against the displacement of a fluid particle. Howard and Gupta[30] extended this stability criterion to vortex flows with axial velocity. His formulation shows that axial velocity shear

acts to lessen the range of stability, but predicts that axial flows are more likely to maintain strong radial shears within regions of strong rotation. These criteria infer that turbulence will be stabilized within the core of a vortex, even if strong gradients of axial velocity are present. On the other hand, turbulence can be enhanced along the outer region of the swirling flow.

Table 1. *Vortex decay mechanisms and their effects.*

VORTEX DECAY MECHANISMS	
Mechanism	**Effect**
Molecular Viscosity	Ineffective for atmospheric vortices – acts to increase vortex core diameter
Ambient Turbulence	Decays vortex from outside inward
3-D Dynamic Instabilities	Bursting (sudden core enlargement) and Crow (vortex linking)
Stratification	Generates opposite-sign vorticity at vortex periphery – vortex decays from outside
Ground	ditto

Since Reynold's numbers are very large and turbulence is suppressed within the central region of the vortex, the core (as defined by the radius of maximum tangential velocity) expands very little with time. Turbulence can be effective outside the core, resulting in a decay process that works inward to remove vorticity from the core.[23] This decay process due to turbulence, as interpreted from Lidar observations of atmospheric vortices, is described further by Hallock and Burnham,[22] and Sarpkaya.[23]

Although vortices weaken over time due to the removal of their vorticity by turbulence, their lifespan may suddenly be shortened by the onset of three-dimensional instabilities. Crow instability occurs when two trailing vortices undergo a sinusoidal instability that grows exponentially until the two vortices link forming a series of crude vortex rings.[29, 31] Once the rings form, the wake quickly weakens into a less harmful state.[31] Vortex lifespan, defined as the time period until linking takes place, is believed to be influenced by atmospheric turbulence, stratification, and wind shear.[10, 24, 32] A comprehensive and validated relationship for vortex lifetime, based on the correlation between atmospheric state variables and the onset of Crow instability, may be useful to include in an AVOSS system. A list of the decay mechanisms and their effect on atmospheric vortices is shown in Table1.

II. NUMERICAL WEATHER FORECAST

The AVOSS predictor model is currently being developed to use observed atmospheric state parameters. The utility of the predictor model can be increased if short term forecast of essential weather parameters are provided. In order to meet this need an existing mesoscale numerical weather forecast model is being tailored for short-term operational forecast in the terminal area.

Under a cooperative agreement with NCSU, the Mesoscale Atmospheric Simulation System[33, 34] (MASS) model is being adapted to run as a portable operational system that will meet weather requirements of an AVOSS predictor system. The model is a 3-dimensional, hydrostatic, terrain-following numerical weather prediction model, and is initialized from comprehensive 3-dimensional data sets that include nation-wide rawinsonde observations, surface measurements, satellite derived measurements, and atmospheric wind profiler data. The model includes boundary-layer and radiation physics, cumulus parameterization schemes, and a high-resolution terrain data base. Fine-resolution terminal area forecast with horizontal grid sizes between 7.5 km to 15 km can be realistically achieved in an operational setting via one-way nesting procedures. The model has been used both operationally[35] and for scientific research since 1979 under other NASA programs at GSFC, MSFC, KSC, and LaRC. The MASS model will be able to generate vertical profiles of wind speed and direction, wind shear, temperature, and turbulence, as well as ceiling and cloud cover products, and precipitation forecast. Final choice of the model domain size and resolution will be determined such that it can produce operational forecast on current state-of-the-art workstations.

Currently MASS model simulations are being compared with observed data sets from the 1995 Memphis deployment.[36] Results are highly encouraging, demonstrating its ability to resolve and accurately predict the development of low-level jets and small-time scale events. Our intention is to run MASS in real time for DFW starting this summer and evaluate its operational capability for supporting an AVOSS system.

III. Wake Vortex Modelling

Numerical modelling of wake vortices is a very challenging research area. At a minimum, accurate and nondissipative numerical techniques, proper treatment of turbulence, and realistic initial conditions are necessary. Direct Numerical Simulation (DNS) of 3-D wake vortex flows are limited to low Reynolds numbers, and thus may not give an accurate representation of atmospheric wake vortices. Reynold's averaged Navier Stokes (RANS) simulations are usually based on closure approximations derived from ordinary boundary-layer shear flows and have dubious validity when extended to rotational flows. The large eddy simulation (LES) approach allows the direct numerical simulation of all turbulence scales that are resolvable by the grid and depends only on closure models for the subgrid scales. The LES approach is probably the better method for achieving the most realistic simulations of atmospheric wake vortices. The numerical model should also have a meteorological frame work, at least if one believes that wake vortex behavior is dependent upon atmospheric parameters. Whatever approach is decided upon, the researcher should put special emphasis on validation with vortex flows that are observed in the atmosphere.

Previous numerical modelling studies of aircraft wake vortices are numerous and will not be reviewed here. Recent studies have used: two-dimensional laminar or DNS,[37, 38, 39] three-dimensional DNS,[40, 41] two-dimensional RANS,[42] two-dimensional LES,[43] and three-dimensional LES.[44, 45, 46]

In order to better understand wake vortex behavior and develop relationships with environmental parameters, numerical modelling is being carried out with the Terminal Area Simulation System[47, 48] (TASS) in both two and three dimensions.

TASS Model Description

TASS is a LES model with a time-split compressible, non-Boussinesq equation set. It has a meteorological reference frame and is able to simulate a wide range of atmospheric conditions that include vertical wind shear, stratification, turbulence, fog, and precipitation. The model includes parameterizations for ground stresses that are a function of surface roughness, allowing for realistic ground interactions. The TASS model was initially developed to study microburst and cumulonimbus convection for the NASA-FAA windshear program[49, 50] and it has been adapted to study other phenomenon, including wake vortices. Model options exist for either two or three dimensions, and for lateral boundary conditions, which can be either periodic or open-nonreflective. Top and bottom boundary conditions can be chosen as either closed (with no-slip conditions at the ground) or periodic.

The TASS model consists of 12 prognostic equations: three equations for momentum, one equation each for pressure deviation and potential temperature, six coupled equations for continuity of water substance (water vapor, cloud droplet water, cloud ice crystals, rain, snow and hail) and a prognostic equation for a massless tracer. The model also contains numerous microphysics models for computing cloud and precipitation physical interactions. Subgrid closure is achieved by a conventional Smagorinsky formulation that has been modified for Richardson-flux dependency. The prognostic equations are approximated using 4th order energy-conserving space differencing and 2nd order time differencing. Only light numerical filtering is applied using a 6th-order filter. The formulation is stable for long term integrations and is essentially free from numerical diffusion.[51] Further details of the model formulation can be found in references [47 and 48].

Vortex Initialization

The initial wake vortex field for either two- or three-dimensional simulations is specified with a simple vortex system that is representative of the post roll-up, wake-vortex velocity field. The vortex system is initialized with the superposition of two counter-rotating vortices. The TASS model offers a choice of vortex models including: Rankine [Saffman,[52] pg. 22], Lamb [Saffman,[52] pg. 253] , Burnham-Hallock,[11] and a recently added model described below. Mostly, we have used the Burnham-Hallock model which has a tangential velocity, V, according to:

$$V(r) = \frac{\Gamma_\infty}{2\pi}\frac{r}{r_c^2 + r^2}$$

where, r_c is the core radius, and Γ_∞ the circulation at $r >> r_c$. A new model (which is based on Lidar observations of several wake vortices measured early in their evolution) is represented as:

$$V(r) = \frac{\Gamma_\infty}{2\pi r}\left(1 - \exp\left[-11.8826\left(\frac{r}{B}\right)^{0.75}\right]\right)$$

where B is the span of the generating aircraft. The above formula is applied only at $r > r_c$ and is matched with a Lamb model profile for $r < r_c$. Coincidentally, both the above formula and the Burnham-Hallock model give

nearly identical results for $r > B/10$, if r_c is chosen as 3.75% of span. The values assumed for initial vortex separation and circulation are derived from an aircrafts weight, span, and airspeed according to conventional formula based on elliptical loading; i.e., $b_o = \pi B/4$, and $\Gamma_\infty = 4Wg/(\pi B \rho V_a)$. Appropriate vortex image conditions are applied to the initial wake field to ensure consistency and mass continuity at the model boundaries. For three-dimensional runs the initial vortex pair is assumed to be uniform along the vortex axis.

As an example of this vortex initialization procedure, a DC-10 wake is simulated by providing the known weight, airspeed, and span for a DC-10. Other inputs would include vortex core radius and generating altitude. Validation test have shown this approach to be adequate for wake vortex initialization.

Ambient Conditions and Other Initial Input

The TASS model is constructed to be applicable to many atmospheric phenomenon without special considerations to changing internal parameters. Ambient conditions for temperature, wind, humidity and condensed water (if any) are initialize with vertical profiles. Other inputs include grid size, surface roughness, latitude, surface heat flux parameters (for atmospheric boundary layer simulations), and boundary condition options. Currently, terrain is not considered and horizontal variations in the mean ambient fields and surface roughness are ignored.

Approach for Wake Vortex Modelling

As mentioned earlier, both 2-D and 3-D simulations are being run with the TASS model. The 2-D option can be used to simulate high-resolution fields with minimal use of computer time, and thus can run with very- fine grid sizes. Typically, uniform grid sizes between 0.5 m and 1 m are used. The 2-D version has been found to be an excellent tool for examining wake vortex transport vs meteorology, as well as studying wake vortex interaction with the ground. Case study validations can be found in references [18, 48]. The disadvantage of using the 2-D option is that it cannot realistically simulate vortex decay. The resolved-scale turbulence is two-dimensional with energy cascading upscale rather than downscale as with 3-D turbulence; i.e., turbulent eddies unable to contract by stretching, coalesce with other eddies and grow in size. The unrealistic properties of two-dimensional turbulence results in an underestimation for the rate of vortex decay. Other disadvantages of the 2-D system are that it does not permit three-dimensional coupling between axial and tangential flow, and obviously does not permit the growth of 3-D instabilities.

TASS is also being used with two different three-dimensional approaches. One approach is to assume periodic lateral boundaries as was done in many of the recent studies. [40, 44, 45] In this approach, a Kolmogorov spectrum of resolved-scale turbulence is initialized and maintained by an artificial external forcing. Once the turbulence becomes steady, a wake vortex pair is specified uniformly along the length of the model domain. The advantages of this approach are its ease to implement and its capability for vortex interaction with fully three-dimensional turbulence. This approach also allows for the study of vortex decay and its sensitivity to various intensities of ambient turbulence. The disadvantages are that it implies that the vortex has infinite length (prior to linking) and that the vortex ages (decays) at roughly the same rate for all positions along the vortex.

In the second of the TASS 3-D approaches, the domain moves with the speed of the generating aircraft and the initial wake-vortex field is held fixed on the upstream or forward boundary. The remaining lateral boundaries are open and allow the wake vortex to propagate outward with minimal undue influence. An illustration of this approach can be found in Schowalter et al.[53] The advantage of this method is that it allows the simulation of a "true" trailing vortex that gradually ages as you move downstream from the forward boundary. This approach allows coupling between the older and newer sections of a vortex, which may influence the axial flow structure. The disadvantage of this method is that it is more difficult to implement an ambient field of resolved-scale turbulence. Zoning methods have been developed for TASS that increase the computation efficiency of this approach,[54] and eventually the model will run with a series of nested grids that link the fine-scale domain with a more course resolution domain in which atmospheric boundary layer turbulence is allowed to "grow." Validation of the ability for TASS to grow a turbulent boundary layer has already been achieved,[55, 56, 57, 58] and the development of grid nesting procedures are underway.[59, 60] The turbulent atmospheric boundary layer studies in addition to providing realistic turbulence fields for 3-D vortex simulations, may also be useful in helping to understand how turbulence profiles can be obtained or approximated from limited measurements.

The sensitivity between each of the above approaches was tested, assuming no ambient turbulence

and with otherwise identical settings. There were only minor differences between the 2-D simulation and the two 3-D approaches (excluding differences in axial velocity). The addition of resolved-scale turbulence, however, greatly increased the differences between the 3-D and 2-D simulations.

IV. TASS Simulation Results

In this section some of the TASS simulation results are briefly described.

Fog and Rain Effects on Wake Vortices

At the request of the NASA-LaRC radar group, who are evaluating the feasibility of radar for detection of wake vortices,[61] a TASS-generated data set was requested for a fog environment. Several TASS 2-D cases were run for a C-5A generated wake within a fog environment which was observed at Vandenberg, CA. No ambient turbulence or crosswinds were assumed. Figure 2 is from one of the simulations, showing the depletion of fog along and underneath the flight path. Sinking air within the center of the vortex oval, heats due to compression and quickly evaporates any suspended fog droplets. Along the vortex periphery where rising motion occurs, the fog water content is slightly enhanced as condensation occurs in the rising air. As shown in fig. 3, similar clear slots occur behind aircraft in actual fog environments.

Table 2. *Environmental parameters for fog and rain sensitivity cases.*

Condition	Liquid Water ($g\ m^{-3}$)	Visibility (nm)	Radar Reflectivity (dBZ)
dry	0	-	-
fog	0.2043	0.09	-
rain	0.2043	5	30
rain	0.425	3	35
rain	2.4	0.9	46

A second series of 2-D simulations were carried out by Switzer[54] to access the sensitivity of fog and rain on wake vortex transport. This series of experiments included a dry baseline cases, a fog case, and three rain cases (table 2). Heavy fog and rain were not included in the experiments since such conditions would likely force the closure of an airport due to poor visibility. The ambient conditions assumed no wind or turbulence and a temperature lapse rate close to moist-adiabatic. For this lapse rate, saturated air parcels would have neutral static stability, while unsaturated air parcel would have stable static stability. The rain and fog environments are specified to be steady and uniform prior to injecting the representative wake vortex pair. Simulated trajectories are shown in figs. 4 and 5. The experiments indicate that rain and fog's affect on vortex trajectory is inconsequential. This implies that wake vortex predictor algorithms need not include moist processes in their transport calculations.

Wake Vortex Sensitivity to Crosswind Shear

The initial motivation for examining crosswind shear effects was from data observed during the Memphis 1994 and 1995 deployments. Following sunset, wake vortices would sometimes either stall or be deflected upwards as they penetrated the region near the interface between the residual layer and developing nocturnal stable layer.[62] The measured values of stratification were too weak to cause the observed levels of deflection. Unfortunately, high-resolution vertical profiles of the crosswind were not always available near the altitude of the observed deflection. We postulated that pronounced shear zones due to change in airmass characteristics existed within this transition region. Such characteristics have been found from other boundary layer observations (i.e., Stull[27]).

In order to investigate the effect of crosswind shear we have run numerous cases with 2-D TASS of different crosswind shear profiles.[18, 63] We found that shear zones and nonlinear changes of crosswind with height could affect vortex descent, but linear profiles of crosswind shear had no affect. Furthermore, Zheng and Baek[64] investigated this effect with an inviscid, kinematic model, having the shear represented by point vortices. They found that the deflection was due to the kinematic interaction between the vorticity of the wake vortices and the vorticity of the crosswind shear.

Presented below are a set of experiments that examine the sensitivity to a shear zone. Five experiments were run with crosswind profiles similar to that represented in fig. 6. A 25 m thick shear zone was centered at 65 m above ground level (AGL). The crosswind profiles contained uniform crosswind above the shear zone and no wind below the shear zone. Four experiments were run with the crosswind above the shear zone varying from 1 to 4 m/s. Also, one baseline case was run with no crosswind at any elevation. The

numerical experiments assume an initial wake vortex pair generated from a B-727 at an altitude of 175 m AGL. The vortex trajectories from these experiments are shown in fig. 7. Note that initially, the vortices translate with the uniform crosswind. But, as the vortices encounter the shear zone they may be deflected depending upon the magnitude of crosswind change. For the cases having a crosswind change less than 3 m/s, the vortices penetrated the shear zone, but descended at a slower speed. For the cases where the crosswind change was 3 m/s or greater, the starboard or downstream (downshear) vortex was deflected upwards. As the vortex separation increased following the deflection, the subsequent mutual interaction between the vortices decreased, leaving the upwind (upshear) vortex stranded near the altitude of the shear zone. Also note from fig. 7 that those vortices that were able to penetrate the shear zone continued to move laterally, even though there was no ambient wind below the shear zone. This is because crosswind momentum from aloft is transported downward with the vortex oval. In all of the cases the ambient wind was calm below 60 m AGL, hence a vortex predictor algorithm that used only near surface wind data would always predict no mean lateral movement. This emphasizes the need for a detailed knowledge of the wind structure with height for an AVOSS type system.

Table 3. *Sign of crosswind vorticity vs vortex with highest bounce*

Case	$\partial U/\partial z = \omega$	$\partial^2 U/\partial z^2 = \partial\omega/\partial z$	Vortex with Highest Bounce
No shear	0	0	same
Linear shear	+	0	same
Nonlinear shear	+	-	downshear
Nonlinear shear	+	+	upshear

The relationship between shear and which vortex is acted upon the greatest (or most likely to rise) is summarized in Table 3 from a number of TASS simulations. As indicated in Table 3, the bounce of the vortex is related to the vertical change in ambient shear (i.e. $\partial^2 U/\partial z^2$) rather than the shear alone. The TASS experiments demonstrate that vertical changes in the along-track component of ambient vorticity (nonlinear shear) can preferentially reduce the descent rate of vortices, and may lead to vortex tilting and vortex rising. Linear shear (constant ambient vorticity) has no impact on the vortex descent rates.

Effect of Stratification on Vortex Structure

In order to assess how stable stratification may affect the structure and decay of a wake vortex, a three-dimensional experiment was conducted using the open lateral boundary approach. The initial conditions for this experiment are described in Schowalter et al[53] and assume a DC 10-10 aircraft with a normalized Brunt-Vaisala frequency of $N^* = 1$. The initial ambient state is assumed to be quiescent, thus both members of the vortex pair decay at the same rate. The initial vortex separation, b_o, is 36 m, and 15.6 s is equivalent to one nondimensional unit of time ($t^* = 1$).

In the simulation the vortex pair descends until it stalls at 35 s (t^* slightly greater than 2). During this time period, the vortex pair descends to a depth of slightly greater than b_o. As the vortex pair descends within this very stable environment, the vortex oval heats due to adiabatic compression and produces buoyancy forces which mitigate the weaker tangential velocity at the outer radii of each vortex. The weakening of the circulation at the outer radii, lessens the mutual interaction between each vortex causing the vortices to stall.

Evolution of the circulation profiles in Fig. 8. show that the circulation is quickly eaten away at the outer radii. By t = 32 s, the circulation is confined to radii less than b_o. After this time the vortex continues to shrink as it is eaten away from the outside. Meanwhile, the circulation within 15 m of the vortex center, which is closely related to the hazard,[65] shows only slight decay until after 48s, well after the time in which the vortex has stalled. Following this time the inner circulation decays rapidly. Rayleigh instabilities can be generated in the region where circulation decreases with radius, and may aid in the decay of the vortex.

This simulation illustrates how stratification can alter the circulation profile of a vortex, causing it to decay from the outside. Also one may infer that an AVOSS predictor algorithm may need to compute the decay of circulation at least for two different radii, since the circulation at the outer radii affects vortex transport and the circulation at smaller radii affects the hazard the vortex would pose to an encountering aircraft.

Influence of 3-D Ambient Turbulence on Decay

Han et al[66, 67] have run a set of 3-D TASS simulations in order to examine the influence of ambient turbulence on wake vortex structure and lifetime. Their results are summarized in this section.

The 3-D periodic approach is taken for these simulations with perodic lateral and vertical boundaries. The ambient conditions assume neutral stratification, no wind or humidity, and a kolomogorov spectrum of resolved-scale turbulence which is close to statistical isotropy. Experiments were conducted for five values of nondimensional turbulence dissipation, ranging from: $\epsilon^* = 0.0322$ to 0.584. These values represent realistic intensities ranging from weak to strong turbulence. Once the turbulence became statistically stable a vortex pair was injected into the domain of the simulation. The domain size used for each of the simulations was: $20b_o \times 5b_o \times 5b_o$ resolved by grid sizes of $b_o/16$, $3b_o/64$, and $3b_o/64$, in the longitudinal, lateral, and vertical directions, respectively. In each case, the core radius was assumed to be $b_o/16$. [The actual simulations were run with dimensional variables with b_o equal to 32 m.] More detail regarding the initialization can be found in Han et al.[66]

Figure 9 shows the top and side views of the wake-vortex pairs at three nondimensional times and at three turbulence intensities. The visualization of the vortices are achieved using a similar technique as in Corjon et al.[68] The three turbulence levels depicted are for ϵ^* equal to 0.068, 0.143 and 0.50; representing, weak, moderate, and strong turbulence, respectively. These values fall within the range of typical atmospheric values as shown in fig. 10. The results in fig. 9 show that stronger turbulence acts to accelerate the onset of crow instability and increase the distortion of the vortices. Wake vortex lifespans, as defined by the time linking takes place, are shown as function of t^* and ϵ^* in fig. 11. The wake vortex lifespan decreases with nondimensional turbulence dissipation, which is consistent with previous studies including Crow and Bate's[29] original analysis and Sarpkaya and Daily's[23, 32] experimental water tank data. As shown in fig. 11, the TASS data more closely agree with Sarpkaya's analytical model[23] than the model of Crow and Bate. With the TASS data in fig.11 and the atmospheric data in fig. 10, our simulation would predict a vortex lifespan for a DC 10-30 (assuming light winds with neutral stratification) to last several minutes in the early morning and less than a ½ minute during the middle of the day.[+] Yet to be examined in this modelling approach are the influence of stratification, wind shear, and non-isotropic turbulence on vortex lifetime.

Figures 12-14 show the normalized circulation profiles at three different times for the case with $\epsilon^* = 0.175$. Also shown are results from a 2-D simulation that had no ambient turbulence. [A 3-D simulation without ambient turbulence would generate a nearly identical profile to that shown for 2-D.] The three times chosen in figs. 12-14 were selected prior to significant distortion due to vortex-linking instability. Comparison of the profiles indicate a slow decrease in circulation with time, with the profile being characterized by a nearly uniform distribution of circulation beyond two core radii. Qualitatively, the circulation distributions are similar in structure to those analyzed by Sarpkaya[23] from Lidar measurements. An example of one of the Lidar profiles is shown in fig. 15. Also, note that the profiles in figs. 12-14 have a different structure than those simulated for the stably-stratified case (fig. 8). The distribution of circulation from the stratified environment decay inward, while those from the unstratified but turbulent environment weaken uniformly at all radii.

Laminar 2-D Simulations

In order to understand what differences that laminar simulations may produce, two additional simulations are carried out assuming a Reynolds number of 1000 and 1 million. TASS with the 2-D DNS option and no ambient turbulence is assumed. The simulations were initialized with observed parameters, so as to compare results with the Lidar measurements from Memphis case 1273. [This particular case was for a DC-10 on approach in an evening environment that was characterized by weak crosswinds and low to moderate turbulence.] The circulation distributions at $t^*=3.6$ are compared with the Lidar measured data in fig. 15. At high Reynold's number the circulation profile decayed very little from its initial state. At a Reynold's number of 1000, the vortex pair decayed by expanding its core. Both simulations indicated very little decay at larger radii. This is in contrast with the observed data and the TASS 3-D LES simulations. This suggest that laminar simulations at low-Reynold's number (whether numerical or experimental) cannot correctly decay atmospheric vortices. The similarity between the high-Reynold's number simulation at $t^*=3.6$ with its initial state, implies

[+]Assuming, Γ_∞=500 m^2/s and b_o = 40 m.

the absence of numerical diffusion in the TASS simulations.

Summary

The progress of the modelling efforts in support of the developing the AVOSS system are making important strides forward. The wake vortex modelling effort is cable of addressing important issues regarding vortex decay and transport, and is providing important guidance the development of an AVOSS system. Both the modelling and recent field studies show that atmospheric effects from wind shear and turbulence have significant influence on vortex transport and decay.

Acknowledgments

This research was sponsored by NASA's Terminal Area Productivity Program. Numerical simulations were carried out on NASA Ames' Cray supercomputers. I would like to acknowledge George Switzer (RTI) and Dave DeCroix, Jongil Han, C.T. Kao, and Shaohua Shen of NCSU for providing a number of the figures that appear in this paper.

References

1. Hinton, D.A., "Aircraft Vortex Spacing System (AVOSS) Conceptual Design," NASA Tech Memo No. 110184, August 1995.

2. Hinton, D.A., "An Aircraft Vortex Spacing System (AVOSS) for Dynamical Wake Vortex Spacing Criteria, "AGARD 78th Fluid Dynamics Panel Meeting & Symposium, Trondheim, Norway, AGARD CP-584, Paper No. 23, May 1996.

3. Perry, R.B., Hinton, D.A., and Stuever, R.A., "NASA Wake Vortex Research for Aircraft Spacing," 35th Aerospace Sciences Meeting & Exhibit, Reno, NV, AIAA Paper No. 97-0057, January 1997, 9 pp.

4. NASA, "The Aircraft Vortex Spacing System (AVOSS)," http://aesd.larc.nasa.gov/avoss/avoss.html, 1998.

5. Robins, E.R., Delisi, D.P., and Greene, G.C., "Development and Validation of a Wake Vortex Predictor Algorithm," 36th Aerospace Sciences Meeting & Exhibit, Reno, NV, AIAA Paper No. 98-0665, January 1998, 10 pp.

6. Campbell, S.D., Dasey, T.J., Freehart, R.E., Heinrichs, R.M., Matthews, M.P., Perras, G.H., and Rowe, G.S., "Wake Vortex Field Measurement Program at Memphis, TN Data Guide," Project Report: NASA/L-2, January, 1997. [Available from NTIS]

7. Campbell, S.D., Dasey, T.J., Freehart, R.E., Heinrichs, R.M., Matthews, M.P., and Perras, G.H., "Wake Vortex Field Measurement Program at Memphis, TN," 34th Aerospace Sciences Meeting & Exhibit, Reno, NV, AIAA Paper No. 96-0399, January 1996.

8. Dasey, T.J., and Heinricks, R., "An Algorithm for the Recognition and Tracking of Aircraft Wake Vortices with a Continuous Wake Coherent Laser Radar," Optical Society of American Coherent Wave Laser Radar Topical Meeting, Keystone, CO, July 1995.

9. Hannon, S., Phillips, M., and Henderson, S., "Pulsed Coherent Lidar Wake Vortex Detection, Tracking and Strength Estimation in Support of AVOSS," NASA First Wake Vortex Dynamic Spacing Workshop, Proceedings, Hampton, VA, NASA CP-97-206235, May 1997, pp. 247-260.

10. Tombach, I., "Observations of Atmospheric Effects on Vortex Wake Behavior," *J. Aircraft*, Vol 10, November 1973, pp 641-647.

11. Burnaham , D.C., and Hallock, J.N., "Chicago Monostatic Acoustic Vortex Sensing System," Report No. DOT-TSC-FAA-79-103.IV, July 1982, 206 pp. [Available from NTIS]

12. Garodz, L.J., and Clawson, K.L., "Vortex Wake Characteristics of B757-200 and B767-200 Aircraft Using the Tower Fly-By Technique, Volumes 1 and 2," NOAA Tech. Memo. ERL ARL-199, Jan. 1993. [Available from NTIS]

13. Rudis, R.P., Burnham, D.C., and Janota, P., "Wake Vortex Decay Near the Ground Under Conditions of Strong Stratification and Wind Shear," AGARD 78th Fluid Dynamics Panel Meeting & Symposium, Trondheim, Norway, AGARD CP-584, Paper No. 11, May 1996.

14. Hallock, J.N., "Vortex Advisory System Safety Analysis, Volume 1: Analytical Model," Report No. DOT-TSC-FAA-78-15.1, September 1978, 160 pp. [Available from NTIS]

15. Zak, A.J. and Rodgers, W.G. Jr., "Documentation of Atmospheric Conditions During Observed Rising Aircraft Wakes," NASA Contractor Report 4767, April 1997, 133 pp.

16. Vicroy, D., Brandon, J., Greene, G., Rivers, R., Shah, G., Stewart, E., and Stuever, R., "Characterizing the Hazard of a Wake Vortex Encounter," 35th Aerospace Sciences Meeting & Exhibit, Reno, NV, AIAA Paper No. 97-0055, January 1997, 7 pp.

17. Liu, C.H. and Ting, L., "Interaction of Decaying Trailing Vortices in Spanwise Shear Flow," *Computers & Fluids*, Vol 15, January 1987, pp. 77-92.

18. Proctor, F.H., Hinton, D.A., Han, J., Schowalter, D.G., and Lin Y.-L., "Two Dimensional Wake Vortex Simulations in the Atmosphere: Preliminary Sensitivity Studies," 35th Aerospace Sciences Meeting & Exhibit, Reno, NV, AIAA Paper No. 97-0056, January 1997, 13 pp.

19. Spalart, P., "Wake Vortex Physics: The Great Controversies," NASA First Wake Vortex Dynamic Spacing Workshop, Proceedings, Hampton, VA, NASA CP-97-206235, May 1997, pp. 33-44.

20. Spalart, P.R., "Airplane Trailing Vortices," *Ann. Rev. Fluid Mech.*, Vol 30, 1998.

21. Zeman, O., "The persistence of Trailing Vortices: A Modern Study," *Phys. Fluids*, Vol 7, January 1995, pp. 135-143.

22. Hallock, J.N., and Burnham, D.C., "Decay Characteristics of Wake Vortices from Jet Aircraft," 35th Aerospace Sciences Meeting & Exhibit, Reno, NV, AIAA Paper No. 97-0060, January 1997.

23. Sarpkaya, T., "Decay of Wake Vortices of Large Aircraft," 36th Aerospace Sciences Meeting & Exhibit, Reno, NV, AIAA Paper No. 98-0592, January 1998, 11 pp.

24. Liu, H.-T., "Effects of Ambient Turbulence on the Decay of a Trailing Vortex Wake," *J. Aircraft*, Vol 29, April 1992, pp 255-263.

25. Dasey, T.J., MIT Lincoln Laboratories, personal communication, 1997.

26. Greene, G.C., "An Approximate Model of Vortex Decay in the Atmosphere," *J. Aircraft*, Vol 23, July 1986, pp. 566-573.

27. Stull, R.B., *An Introduction to Boundary Layer Meteorology*, Kluwer Academic Publishers, 1988.

28. Donaldson, C.duP, and Bilanin, A.J., "Vortex Wakes of Conventional Aircraft," Advisory Group for Aerospace Research & Development, AGARDograph No. 204, May 1975.

29. Crow, S.C., and Bate, E.R., "Lifespan of Trailing Vortices in a Turbulent Atmosphere," *J. Aircraft*, Vol 13, No. 7, 1976, pp. 476-482.

30. Howard, L.N., and Gupta, A.S., "On the Hydrodynamic and Hydromagnetic Stability of Swirling Flows," *J. Fluid Mech.*, Vol 14, 1962, pp. 463-476.

31. Crow, S.C., "Stability Theory for a Pair of Trailing Vortices," *AIAA J.*, Vol 12, No. 8, 1970, pp. 2172-2179.

32. Sarpkaya, T., and Daly, J.J, "Effect of Ambient Turbulence on Trailing Vortices," *J. Aircraft*, Vol 24, No. 6, 1987, pp. 399-404
.

33. Kaplan, M.L., Zack, J.W., Wong, V.C., and Tuccillo, J. J., "Initial Results from a Mesoscale Atmospheric Simulation System and Comparisons with the AVE-SESAME I Data Set," *Mon. Wea. Rev.*, Vol 110, 1982, pp. 1564-1590.

34. Kaplan, M.L., Koch, S.E, Lin, Y.-L., Weglarz, R. P., and Rozumalski, R.A., " Numerical Simulations of a Gravity Wave Event over CCOPE. Part I: The Role of Geostrophic Adjustment in Mesoscale Jetlet Formation," *Mon. Wea. Rev.*, Vol 125, 1997, pp. 1185-1211.

35. Bauman, W.H., III, Kaplan, M.L., and Businger, S., "Nowcasting Convective Activity for Space Shuttle Landings during Easterly Flow Regimes," *Wea. Forecasting*, Vol 12, 1997, pp. 79-107.

36. Kaplan, M.L., Weglarz, R.P., Lin, Y.-L., Langmaid, A., and Hamilton, D., "The Application of Mesoscale Numerical Weather Prediction Models to

the Terminal Area and Examples from Memphis 1995 Field Data," NASA First Wake Vortex Dynamic Spacing Workshop, Proceedings, Hampton, VA, NASA CP-97-206235, May 1997, pp. 430-459.

37. Spalart, P.R., "On the Motion of Laminar Wing Wakes in a Stratified Fluid," *J. Fluid Mech.*, Vol 327, 1996, pp 139-160.

38. Robins, R.E. and Delisi, D.P., "Potential Hazard of Aircraft Wake Vortices in Ground Effect with Crosswind," *J. Aircraft*, Vol 30, March 1993, pp. 201-206.

39. Zheng, Z.C., and Ash, R.L., "Study of Aircraft Wake Vortex Behavior Near the Ground," *AIAA J.*, Vol 34, March 1996, pp. 580-589.

40. Spalart, P.R., and Wray, A.A., "Initiation of the Crow Instability by Atmospheric Turbulence," AGARD 78th Fluid Dynamics Panel Meeting & Symposium, Trondheim, Norway, AGARD CP-584, Paper No. 18, May 1996.

41. Risso, F., Corjon, A., and Stoessel, A., "Direct Numerical Simulation of Trailing Vortices in Homogeneous Turbulence," 34th Aerospace Sciences Meeting & Exhibit, Reno, NV, AIAA Paper No. 96-0802, January 1996, 8 pp.

42. Zheng, Z.C., "The Effects of Atmospheric Turbulence on Aircraft Wake Vortices," 27th AIAA Fluid Dynamics Conference, New Orleans, LA, AIAA Paper No. 96-1954, June 1996, 11 pp.

43. Schilling, V.K., "Motion and Decay of Trailing Vortices within the Atmospheric Surface Layer," *Beitr. Phys. Atmosph.*, Vol 65, May 1992, pp 157-169.

44. Lewellen, D.C. and Lewellen, W.S., "Large-Eddy Simulations of the Vortex-Pair Breakup in Aircraft Wakes," *AIAA J.*, Vol 34, November 1996, pp 2337-2345.

45. Corjon, A., and Darracq, D., "Three-Dimensional Large Eddy Simulation of Wake Vortices. Comparison with Field Measurements," 15th AIAA Applied Aerodynamics Conference, Atlanta, GA, AIAA Paper No. 97-2309, June 1997, 11pp.

46. Gerz, T., and Ehret, T., "Wingtip Vortices and Exhaust Jets During the Jet Regime of Aircraft Wakes," *Aerospace Science and Technology*, Vol 7, 1997, pp. 463-474.

47. Proctor, F.H., "The Terminal Area Simulation System. Volume I: Theoretical Formulation," NASA Contractor Rep. 4046, DOT/FAA/PM-86/50, I, April 1987. [Available from NTIS]

48. Proctor, F.H., "Numerical Simulation of Wake Vortices Measured During the Idaho Falls and Memphis Field Programs," 14th AIAA Applied Aerodynamics Conference, Proceedings, Part-II, New Orleans, LA, AIAA Paper No. 96-2496, June 1996, pp. 943-960.

49. Proctor, F.H., and Bowles, R.L., "Three-Dimensional Simulation of the Denver 11 July 1988 Microburst-Producing Storm," *Meteorol. and Atmos. Phys.*, Vol. 49, 1992, pp. 107-124.

50. Arbuckle, P.D., Lewis, M.S., and Hinton, D.A., "Airborne Systems Technology Application to the Windshear Threat," 20th Congress International Council of the Aeronautical Sciences, Sorrento, Italy, Paper No. 96-5.7.1, September, 1996, 11 pp.

51. Switzer, G.F., "Validation Tests of TASS for Application to 3-D Vortex Simulations," NASA Contract Report No. 4756, October 1996, 45 pp.

52. Saffman, P.G., *Vortex Dynamics*, Cambridge University Press, 1992, 311 pp.

53. Schowalter, D.G., DeCroix, D.S., Switzer, G.F., Lin, Y.-L., and Arya, S.P., "Toward Three-Dimensional Modeling of a Wake Vortex Pair in the Turbulent Boundary Layer," 35th Aerospace Sciences Meeting & Exhibit, Reno, NV, AIAA Paper No. 97-0058, January 1997, 13 pp.

54. Switzer, G.F., "Studies of Wake Vortex Dynamics for the AVOSS Program using Numericl Modeling Techniques," Final Report, Research Triangle Institute, RTI/4500/056-01F, October 1997, 41 pp.

55. Schowalter, D.G., DeCroix, D.S., Lin, Y.-L., Proctor, F.H., Arya, S.P., and Kaplan, M.L., "Turbulent Statistics in the Atmospheric Boundary Layer: a Comparison of Large Eddy Simulation with Observations," Preprints, 11th Symposium on Boundary Layers and Turbulence, Charlotte, NC,

Amer. Meteor. Soc., March 1995, pp. 552-555.

56. Schowalter, D.G., DeCroix, D.S., Lin, Y.-L., Arya, S.P., and Kaplan, M.L., "Planetary Boundary Layer Simulation Using TASS," NASA Contractor Rep. 198325, April 1996, 22 pp.

57. Schowalter, D.G., DeCroix, D.S., Lin, Y.-L., Arya, S.P., and Kaplan, M.L, " The Sensitivity of Large-Eddy Simulation to Local and Nonlocal Drag Coefficients at the Lower Boundary," NASA Contractor Rep. 198310, April 1996, 43 pp.

58. Schowalter, D.S., Lin, Y.-L., and Arya, S.P., "The Evening Transition of the Planetary Boundary Layer: A Case Study," 1st International Conference on Nonlinear Problems in Aviation and Aerospace, International Federation of Nonlinear Analysis, Daytona Beach, FL., May 9-11, 1996, 6 pp.

59. DeCroix, D.S., Schowalter, D.G., Lin, Y.-L., Arya, S.P., and Proctor, F.H., "A Three-Dimensional Nested-Grid Large Eddy Simulation of the Convective Boundary Layer," 12th Symposium on Boundary Layers and Turbulence, Vancouver, Canada, Amer. Meteor. Soc., Paper 8.10, July-Aug 1997.

60. DeCroix, D., Lin, Y.-L., Arya, S., Kao, C., and Shen, C., "Toward Understanding Wake Vortices and Atmospheric Turbulence Interactions Using Large Eddy Simulation," NASA First Wake Vortex Dynamic Spacing Workshop, Proceedings, Hampton, VA, NASA CP-97-206235, May 1997, pp. 109-130.

61. Mackenzie, A.I., "Measured Changes in C-Band Radar Reflectivity of Clear Air Caused by Aircraft Wake Vortices,", NASA Tech. Paper 3671, November, 1997, 80 pp.

62. Matthews, M.P., Dasey, T.J., Perras, G.H., and Campbell, S.D., "Planetary Boundary Layer Measurements for the Understanding of Aircraft Wake Vortex Behavior," 7th Conf. on Aviation Weather Systems, Long Beach, CA, Amer. Meteor. Soc., February 1997.

63. Proctor, F.H., "Two-Dimensional Parametric Studies of Wake Vortex Interactions with the Atmosphere," NASA First Wake Vortex Dynamic Spacing Workshop, Proceedings, Hampton, VA, NASA CP-97-206235, May 1997, pp. 93-108.

64. Zheng, Z.C., and K. Baek, "Shear-Layer Effects on Trailing Vortices," 36th Aerospace Sciences Meeting & Exhibit, Reno, NV, AIAA Paper No. 98-0316, January 1998.

65. Hinton, D.A., and Tatnall, C.R., "A Candidate Wake Vortex Strength Definition for Application to the NASA Aircraft Vortex Spacing System (AVOSS)," NASA Tech. Memo. 110343, September 1997, 35 pp.

66. Han, J., Lin, Y.-L., Schowalter, D.G., Arya, S.P., and Proctor, F.H., "Large-Eddy Simulation of Aircraft Wake Vortices: Atmospheric Turbulence Effects," 12th Symposium on Boundary Layers and Turbulence, Vancouver, Canada, Amer. Meteor. Soc., July-August 1997, pp 237-238.

67. Han, J., Lin, Y., Arya, S., and Kao, C., "Large Eddy Simulation of Aircraft Wake Vortices: Atmospheric Turbulence Effects," NASA First Wake Vortex Dynamic Spacing Workshop, Proceedings, Hampton, VA, NASA CP-97-206235, May 1997, pp. 131-144.

68. Corjon, A. Risso, F., Stoessel, A., and Poinsot, T., "Three-Dimensional Direct Numerical Simulations of Wake Vortices: Atmospheric Turbulence Effects and Rebound with Crosswind," AGARD 78th Fluid Dynamics Panel Meeting & Symposium, Trondheim, Norway, AGARD CP-584, Paper No. 28, May 1996.

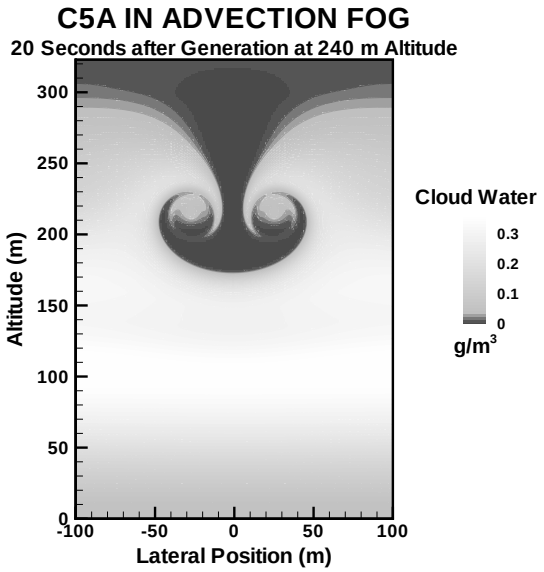

Figure 2. *TASS model simulation of a C5A aircraft in a fog environment.*

Figure 3. *Aircraft vortex interaction with the top of a fog layer. Photo courtesy of the Cessna Aircraft Company.*

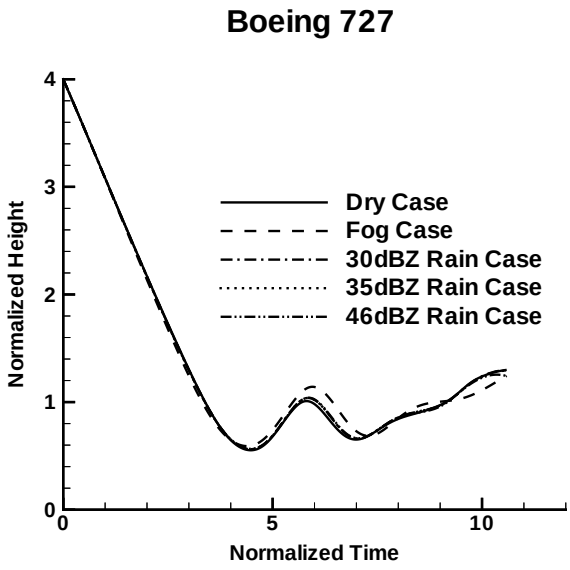

Figure 4. *Vortex height history for TASS model simulation. Height normalized by b_0, vs. t*.*

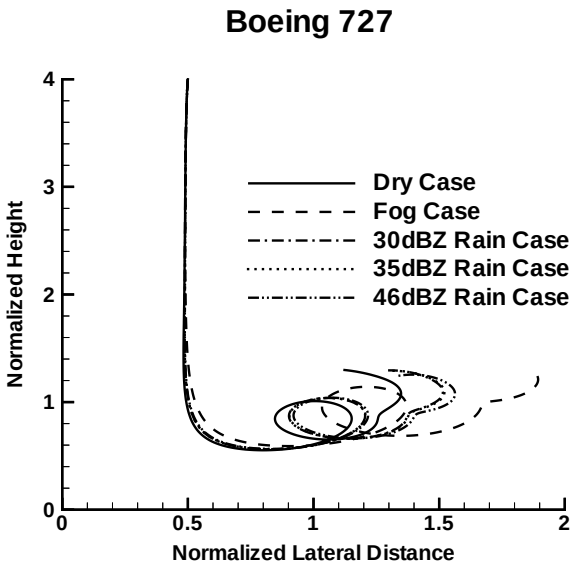

Figure 5. *As in fig. 4, but vortex trajectory comparison. Normalized height vs. normalized lateral distance from flight path.*

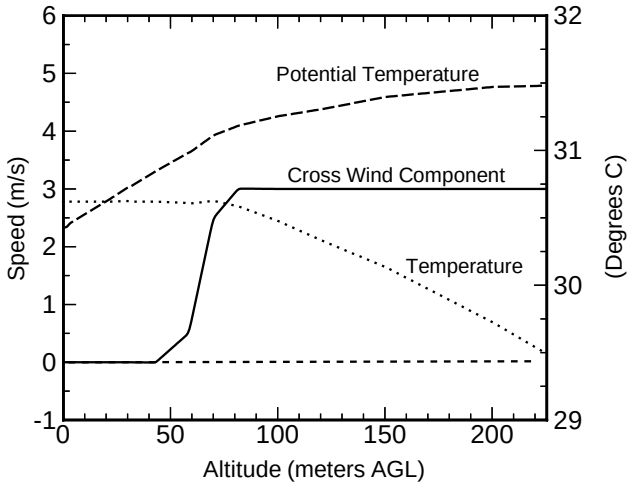

Figure 6. *Initial profiles for ambient temperature, potential temperature, temperature, and crosswind. Only crosswind for 3 m/s case is shown.*

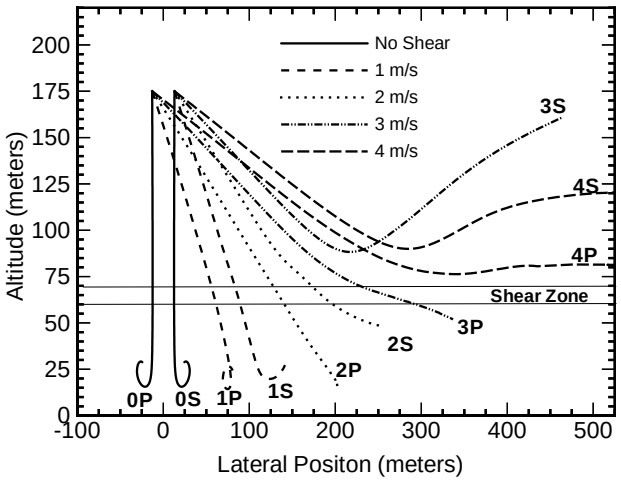

Figure 7. *Trajectories for the simulated wake vortices from the shear-zone experiments. Port (P) and Starboard (S) are shown for each shear profile. [The starboard vortex is downshear from the port vortex.]*

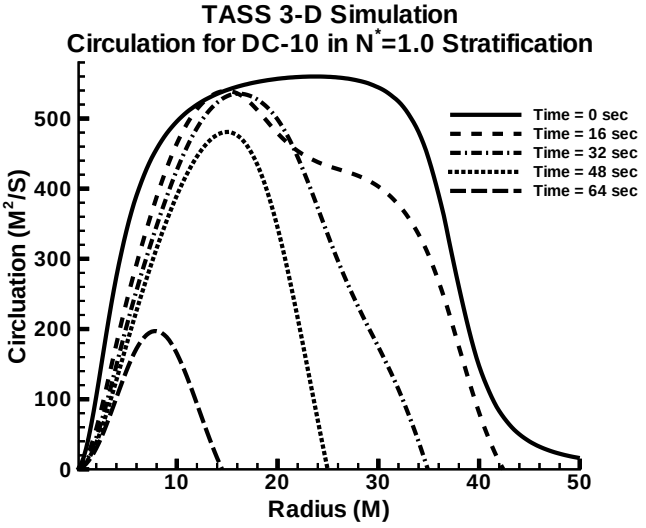

Figure 8. *Radial variation of circulation at several times for the N*=1 case.*

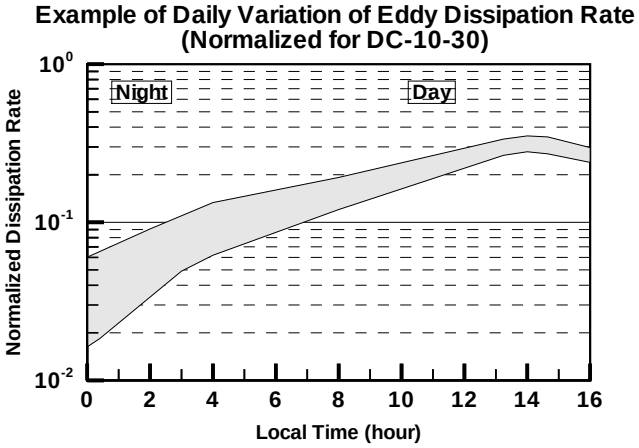

Figure 10. *Typical diurnal variation of ε*. Normalized for a DC 10-30. From measured data during a fair weather day in France during late November. [Adapted from Stull's[27] Fig 5-15.]*

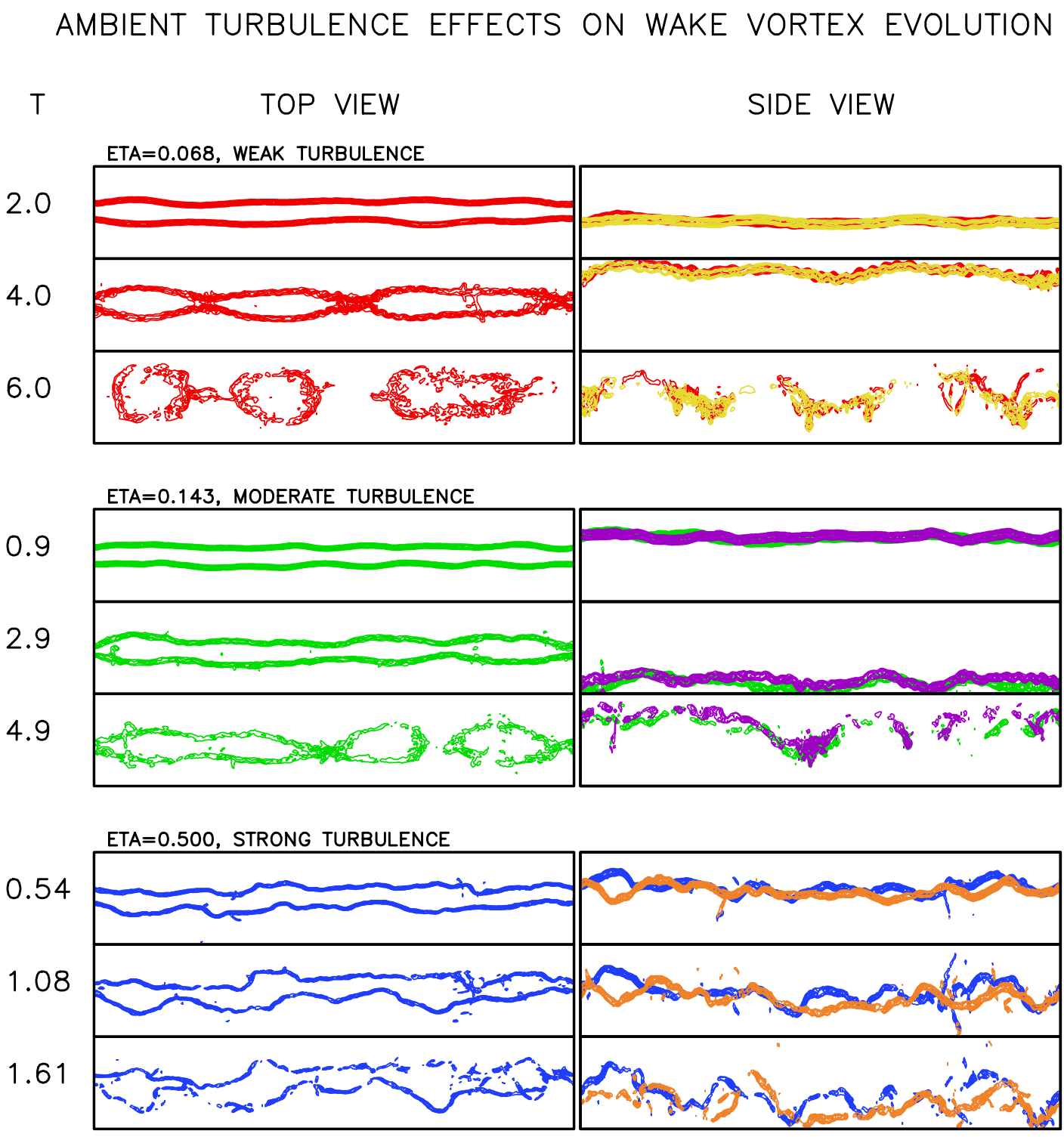

Figure 9. *Top and side view of wake vortex pair for three different turbulence levels (ε*) and three different times (t*). [From Han et al[67]]*

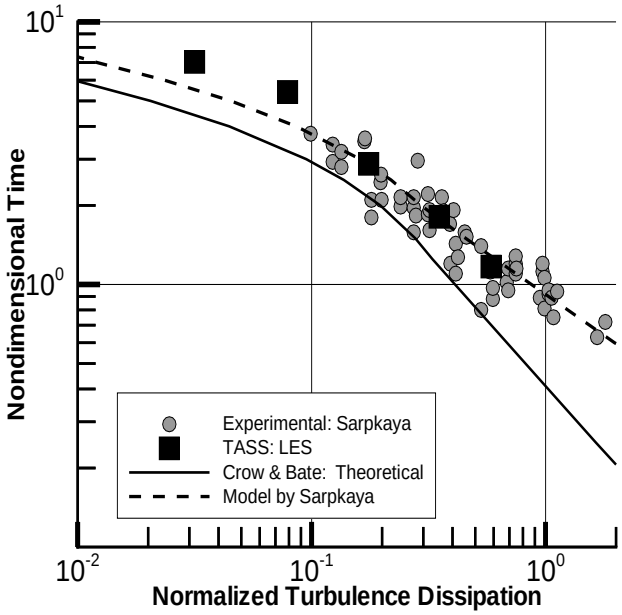

Figure 11. *Vortex lifespan as function of turbulence intensity for a neutrally-stratified atmosphere with no windshear.*

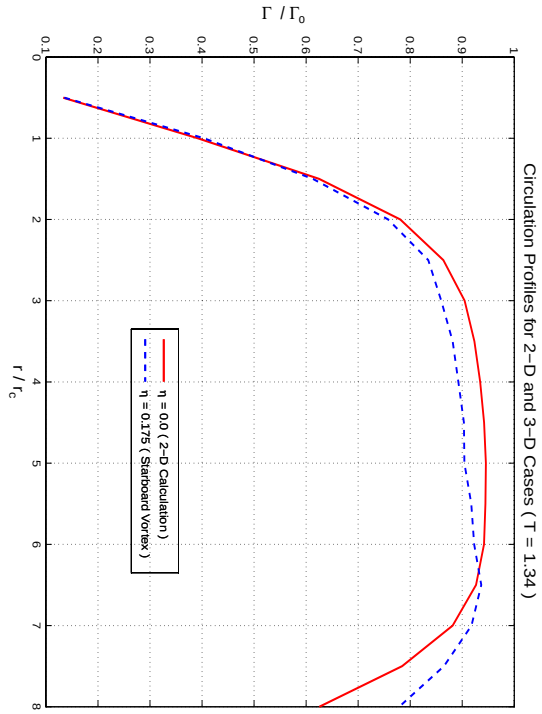

Figure 12. *Radial variation of circulation for ε*=0.175 case for t*=1.34.*

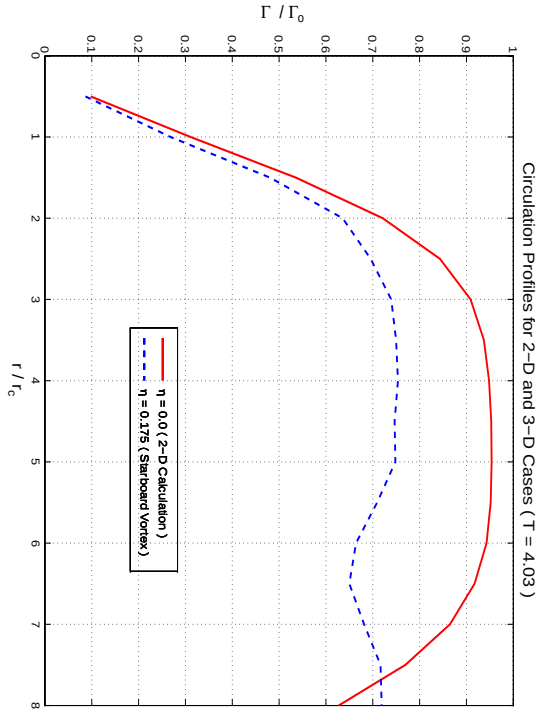

Figure 14. *Same as fig. 12, but for t*=4.03.*

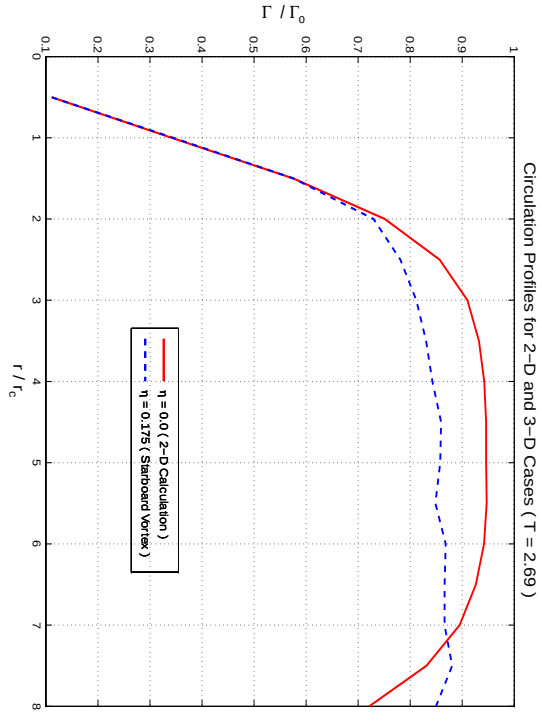

Figure 13. *Same as fig. 12, but for t*=2.69.*

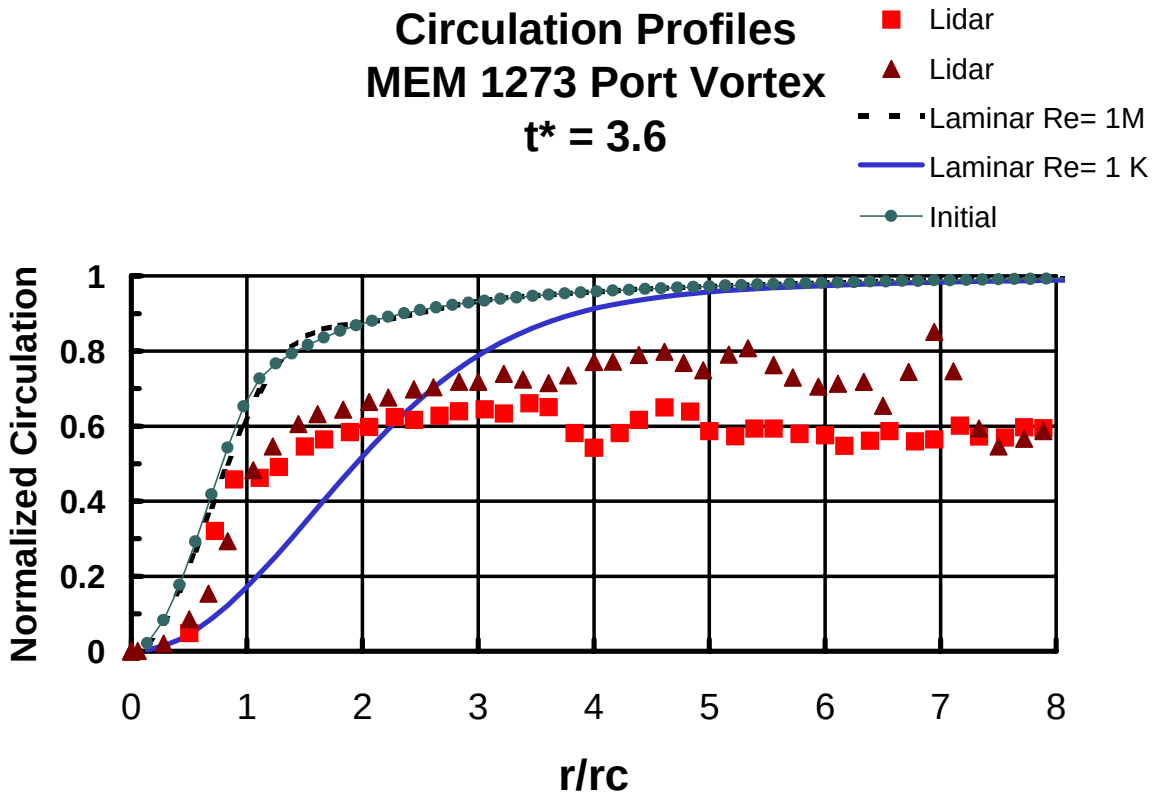

Figure 15. *Radial distribution of normalized circulation (Γ/Γ_∞) for Lidar data and 2-D laminar simulations, at t*=3.6 for a DC 10-30. Radius normalized with initial core radius. Symbols represent Lidar measurements of left and right sides of port vortex. Solid and dashed lines represent laminar simulation with Reynolds numbers of 1000 and 1 million, respectively. Solid line with dots represents the initial profile.*